

Journal Pre-proof

The Impact of the Lamination Pressure on the Properties of Electrospun Nanofibrous Films

Dominik Švára , Barbora Kopřivová , Tomáš Pícek , Petr Mikeš , Anna Kluk , Miroslav Šoóš

PII: S0928-0987(22)00055-0
DOI: <https://doi.org/10.1016/j.ejps.2022.106170>
Reference: PHASCI 106170



To appear in: *European Journal of Pharmaceutical Sciences*

Received date: 3 August 2021
Revised date: 6 March 2022
Accepted date: 17 March 2022

Please cite this article as: Dominik Švára , Barbora Kopřivová , Tomáš Pícek , Petr Mikeš , Anna Kluk , Miroslav Šoóš , The Impact of the Lamination Pressure on the Properties of Electrospun Nanofibrous Films, *European Journal of Pharmaceutical Sciences* (2022), doi: <https://doi.org/10.1016/j.ejps.2022.106170>

This is a PDF file of an article that has undergone enhancements after acceptance, such as the addition of a cover page and metadata, and formatting for readability, but it is not yet the definitive version of record. This version will undergo additional copyediting, typesetting and review before it is published in its final form, but we are providing this version to give early visibility of the article. Please note that, during the production process, errors may be discovered which could affect the content, and all legal disclaimers that apply to the journal pertain.

© 2022 Published by Elsevier B.V.
This is an open access article under the CC BY-NC-ND license (<http://creativecommons.org/licenses/by-nc-nd/4.0/>)

The Impact of the Lamination Pressure on the Properties of Electrospun Nanofibrous Films

Dominik Švára^a, Barbora Kopřivová^b, Tomáš Pícek^a, Petr Mikeš^b, Anna Kluk^c, Miroslav Šoos^{a,1}

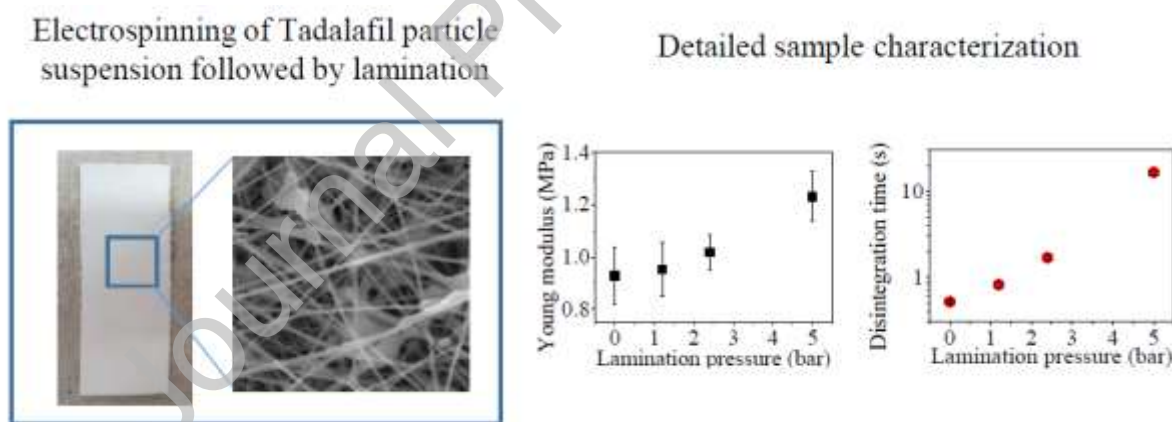
^aDepartment of Chemical Engineering, University of Chemistry and Technology,

Technická 3, 166 28 Prague 6 – Dejvice, Czech Republic

^bDepartment of Physics, Faculty of Science, Humanities and Education, Technical University of Liberec, Studentská 1402/2, 461 17 Liberec, Czech Republic

^cZentiva, k.s., U kabelovny 130, 102 00, Prague 10, Czech Republic

Graphical abstract



Abstract

The purpose of this work is to explore the preparation of nanofibrous orally dispersible films (ODFs) by needleless electrospinning from the active pharmaceutical ingredient (API) Tadalafil using particles suspended in a solution of polymers and other excipients. The prepared films were characterized by a combination of scanning electron microscopy,

¹ corresponding author: miroslav.soos@vscht.cz

mechanical tests, measurements of the disintegration time and dissolution characteristic, X-ray diffraction, and differential scanning calorimetry. Furthermore, we investigated the impact of lamination pressures in the range of 0 to 5 bars combined with films at various relative humidity values on the mechanical properties of the ODF. An increase in lamination pressure resulted in higher Young's modulus values, with the maximum value observed for a sample laminated at a pressure of 5 bar and the maximum stress and strain of the prepared ODF at a lamination pressure of 1.2 bar. Moreover, there was a significant increase in the disintegration time with increase in lamination pressure. The disintegration time ranged from 0.35 s for non-laminated samples to 12 s for samples laminated at a pressure of 5 bar. On the contrary, the lamination pressure did not reveal to have any impact on the dissolution kinetics. These results confirmed that the lamination pressure can improve the processability of ODFs without affecting the API dissolution kinetics.

Keywords: orally dispersible films, electrospinning, particle suspensions, dissolution, particle size, lamination

1. Introduction

One of the problems that affects both small children and the elderly is the usage of oral medications. Tablets and capsules can cause choking problems, while syrups have a shorter shelf life. In addition, many drugs have a bitter taste in the mouth. To reduce these drawbacks, orally dispersible films (ODFs) were introduced as a new type of oral dosage form. The ODF is a relatively new and promising pharmaceutical dosage form. The European Pharmacopoeia defines an ODF as "*single or multilayer sheets of suitable materials, to be placed in the mouth where it disperses in 30 s*" (EDQM, July 2019). In addition to its fast disintegration, other advantages of this form are accurate dosing, rapid onset of action, easy

and discreet application, and no need for water during swallowing (Borges et al., 2015; Bukhary et al., 2018; Hoffmann et al., 2011; Illangakoon et al., 2014). For this reason, this dosage form is suitable for patients with difficulty swallowing (dysphagia), especially for old people or small children (Orlu et al., 2017; Preis, 2015; Slavkova and Breitzkreutz, 2015; Visser et al., 2017). However, a disadvantage of these films remains the limited dose of the drug, which is up to 100 mg (Borges et al., 2015), when considering fibers composed of a solid drug solution in a suitable polymeric matrix. Furthermore, because of the porous structure, ODFs are sensitive and quickly disintegrate in contact with water, and therefore they need to be protected against humidity by high-barrier packaging. As a result of hygroscopicity, the parameters of manufacturing methods and the mechanical strength of the produced films have to be carefully monitored.

The methods used for the production of ODFs include hot-melt extrusion (Jani and Patel, 2015), solvent casting (Pechová et al., 2018), printing methods (Alomari et al., 2015; Alomari et al., 2018; Buanz et al., 2015; Buanz et al., 2011; Feng et al., 2021; Vanaei et al., 2021), and recently introduced electrospinning (Bukhary et al., 2018; Illangakoon et al., 2014; Li et al., 2013; Nagy et al., 2010). Hot-melt extrusion and its application for printing filament production are based on the melting of a drug in a suitable polymer. Although fairly simple to use, high temperatures during processing can cause degradation of a drug or an excipient. The method of solvent casting reduces this limitation; however, it requires the dissolution of compounds in a suitable solvent and thus allowing the formation of a film followed by solvent evaporation (Lang et al., 2014). The nonporous nature of the formed films or the presence of a residual solvent are some of the drawbacks of this method.

In contrast to the methods mentioned above, electrospinning produces highly porous nano/microfiber structures with a large specific surface area (Arinstein, 2017). Typically, a drug is molecularly dissolved in a suitable solvent together with an appropriate polymer

(Cheng et al., 2020; Nagy et al., 2010). The porous structure of the film (Vasvári et al., 2018) can improve the rate of dissolution of the film coupled with the release of the drug substance (Akhgari et al., 2017). Apart from the application of high voltage as an external force to create the Taylor cone (Lukas et al., 2008), several other needless electrospinning setups are used for the production of nanofiber membranes based on the application of magnetic field (Yarin and Zussman, 2004), ultrasound (Nieminen et al., 2018) or high-pressure gas. Despite all these efforts, more work needs to be done for the preparation of nanofiber membranes using drug particle suspensions (Illangakoon et al., 2014; Mikeš et al., 2020) to improve drug loadings. Furthermore, the proposed method does not use toxic organic solvents, such as chloroform, dichloromethane, or acetone, typically used to molecularly dissolve the drug during nanofiber preparation by electrospinning (Lian and Meng, 2017; Oliveira et al., 2013; Zeng et al., 2003).

Therefore, the aim of this work is to prepare nanofiber films using drug particle suspensions and characterize their properties. Due to the uneven thickness of the prepared films, and thus possible heterogeneity in the drug content, the lamination under various pressures was examined. The techniques employed in this study include mechanical strength testing, scanning electron microscopy, dynamic scanning calorimetry, X-ray diffraction, solubility measurement, and optical microscopy. The determination of disintegration time is another important test for the characterization of pharmaceutical formulations. However, the standard approaches, including disintegration testing (EDQM, July 2019; Silva et al., 2018), magnetic resonance imaging (MRI) (Dvořák et al., 2020; Quodbach et al., 2014), or methods based on the addition of water to a sample, i.e. the rotating Petri dish method and the slide frame method (Speer et al., 2018), were not suitable for measurement due to the fast disintegration of ODFs prepared in this work. Therefore, a new method based on optical video microscopy has been developed for determining the disintegration time.

2. Materials and Methods

2.1. Materials

The chemicals used for the preparation of the samples were polyethylene oxide (PEO) with a molecular weight of 100 kDa from Sigma Aldrich (Germany), hydroxypropyl methylcellulose (HPMC E5) from JRS Pharma (Germany) with a molecular weight of 28.7 kDa. Sucrose, sucralose, sodium lauryl sulfate (SDS), and spearmint aroma were purchased from Sigma Aldrich (Germany). Isopropanol (IPA) with a purity of 99.5% was purchased from Penta Chemicals (Czech Republic). Tadalafil, kindly provided by Zentiva k.s., was used as a model drug to examine the effect of the formulation on its behavior. It is used to treat erectile dysfunction, benign prostatic hyperplasia, or pulmonary arterial hypertension, and its formulation in ODFs would be of practical interest. It belongs to the BCS II class of drugs and has pH-independent solubility in water media. Inorganic salts were used to maintain a set value of humidity. The chosen salts were KCl (85% R.H.), NaNO₂ (60% R.H.), and MgCl₂ (32% R.H.). All salts were purchased from Penta Chemicals (Czech Republic).

2.2. Methods

2.2.1. Preparation of suspension for electrospinning

The polymer matrix for the production of ODFs with Tadalafil contained two water-soluble polymers HPMC E5 and PEO. Other excipients were sugars, a flavor to mask the bitter taste of Tadalafil, and SDS as a solubilizer. The liquid polymeric formulation was prepared by dissolving SDS and sugars in a mixture of water and the IPA (the ratio of water to IPA was 1:1). After the dissolution of these two components, the polymers were added to the solution, followed by their dissolution. The mixture after this step increased its viscosity from that of water to approximately 585 mPa.s, as measured by a FungiLab Alpha from Fisher Scientific (USA) rotary viscometer with an L3 spindle operated at 100 RPM at room temperature.

Micronized Tadalafil having D(90) equal to 8 μm as measured by a Mastersizer 2000 (Malvern UK), was then added to the mixture in the form of particles. To ensure good dispersion of drug particles, the mixture was stirred over a period of 12 hours using a magnetic stirring plate operated at 300 RPM. The suspension was measured with a multifunctional device Multi 340i from WTW (Germany) to check the sufficient conductivity of the polymeric liquid suspension, while the pH of the suspension was measured using an EDGE pH meter from Hanna Instruments (Italy). The obtained values of conductivity and pH were equal to 127 $\mu\text{S}/\text{cm}$ and 8.25 (22.9 $^{\circ}\text{C}$), respectively. The exact composition of the ODF is given in Table 1. Before electrospinning, the spearmint flavor was added to the solution.

Table 1 – The composition of the polymer solution for preparing the ODF by electrospinning method. The mass of one strip is approximately 60 mg.

Ingredient	Ratios of components [w/w]	Ratios of dry film [%]	Mass in strip [mg/strip]	Function
Tadalafil	0.075	30.9	18.54	API
HPMC E5	0.058	24.0	14.40	Polymer
PEO 100.000	0.025	10.3	6.18	Polymer
Sucrose	0.083	34.3	20.58	Sweetener
Sucralose	0.001	0.25	0.15	Sweetener
Sodium dodecyl sulfate	0.001	0.25	0.15	Solubilizer
Spearmint	0.006	-	-	Aroma
Isopropyl alcohol	0.375	-	-	Solvent
Water	0.365	-	-	Solvent

The composition of the particular polymer matrix resulted from optimizing different polymers and solvent systems. Among other polymers, hydroxypropyl cellulose (HPC) and polyvinylpyrrolidone (PVP) were also tested. However, both polymers showed lower productivity and worse homogeneity than the selected polymer mixture. The solvent system was selected to avoid complete dissolution of the API, ensuring the electrospinning of the drug particle suspension. Furthermore, attention was focused on the lowering of the water surface tension, as low surface tension is an important parameter for the electrospinning process. The solvent ratio of 1:1 was selected as the optimum after detailed tests, particularly

because of the high productivity. The HPMC:PEO ratio (7:3) was applied for the same reason. Any major change in the composition of these components leads to the reduction of nano/microfiber production, a lower basis weight, and a lower API content of the film.

2.2.2. Nanofiber films manufactured by electrospinning

The Nanospider NS 1WS500U electrospinning equipment from Elmarco a.s. (Czech Republic) was used to produce ODFs containing Tadalafil microparticles. A positive voltage was applied to the wire (spinning electrode) and a negative voltage to the collector; the potential difference was 50 kV. The distance between the spinning electrode and the collector was maintained at 140 mm. The temperature during the experiment was $22\text{ }^{\circ}\text{C} \pm 5^{\circ}$ with a relative humidity of 18.5-22.0 %. A polypropylene spun bond was used as a fabric carrier for electrospinning. Further information about the device configuration is available in Table 2. The resulting layers were packaged in airtight containers immediately after their production to prevent drying of the nanofiber sample.

Table 2 -The process parameters using a Nanospider for the production of ODF.

Voltage [kV]	40 (positive electrode)/-10 (collector)
Electrode distance [mm]	140
Cartridge speed [mm/sec]	430-470
String length [mm]	450
Rewinding speed [mm/min]	10

The electrospinning procedure used during the development of the formulation resulted in films with an uneven thickness (thicker in the center and thinner in the periphery), and thus possibly different drug content of the ODFs. Therefore, lamination was applied to maintain

the desired dosage of the active ingredient. The procedure was performed as described pictographically in Figure 1. The layers were laminated at various pressures (0.3-5 bar) on a Powerbond laminator from Reliant Machinery (UK) at 22 °C with a relative humidity of 20.0 % and a gap clearance equal to 0.1 mm. This procedure also represents an easy way to increase the API content of a strip for a defined area as well as increase the mechanical strength required for further processing.

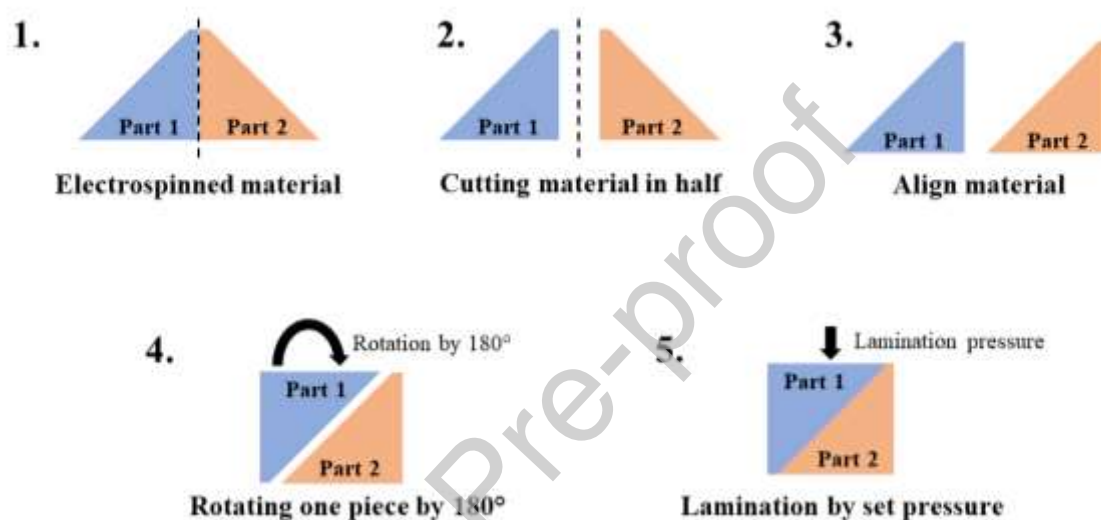


Figure 1 – The diagram of the lamination process. Step 1 – The electrospun sample is divided into two parts. Step 2 – The longitudinal sample is cut. Step 3 – The parts alignment. Step 4 – One part is rotated by 180° and placed on the second part. Step 5 – The parts are laminated by lamination pressure.

The goal of the formulation was to prepare strips with a size of 32.0×25.0 mm and a mass of approximately 60 mg containing around 18.5 mg of Tadalafil. This amount corresponds to the therapeutic dose for an average adult man. If required, the size of the strip was adjusted according to the analytical method. If not stated otherwise, all samples were stored prior to measurement in a desiccator at a maintained temperature of 20 ° C and 50 % of relative humidity. The humidity and temperature were monitored during storage.

2.2.3. Scanning electron microscopy (SEM)

Because of the low conductivity of the prepared samples, they were coated with a thin layer of gold prior to analysis. The samples were prepared for coating at a temperature of 20 °C and 50% relative humidity. The coating process was done with a sputter Emitex K550X from Emitech (UK). The coating current was set to 2.4 mA and the coating time was 2 min. Fibers were analyzed by scanning electron microscopy (Tescan VEGA3 SB, Czech Republic) and the fiber diameters were measured with ImageJ software with the DiameterJ plugin, developed to analyze nanofiber mat samples (Hotaling, 2016; Hotaling et al., 2015). The segmentation of the fiber images was done by applying the segmentation algorithm (M7) to all the samples. The particle size was analyzed with ImageJ software.

2.2.4. Mechanical properties

The measurement of mechanical properties was done with a CT3 texture analyzer CT3 from Brookfield Ametek (USA) equipped with probe clamps TA-DGF001 to measure the tensile strength of film samples. The samples were cut into a rectangular shape with dimensions of 32.0×12.5 mm. Each sample was weighed and the thickness was measured with a micrometer caliper. Samples were measured at six places at the edges of the films that would be in contact with clamps to minimize the effect of sample thickness on the mechanical properties near the center. Each sample was measured with a sampling rate of 100 points/s and a strain rate of 1 mm/s. The measurement of each sample was repeated five times. All measurements were made at 20°C and 50% of relative humidity.

To investigate the impact of storage conditions on the mechanical properties of freshly prepared ODFs, the samples were placed in desiccators with saturated salt solutions to ensure constant humidity. The appropriate salt was chosen to maintain the set humidity value within the desiccator. The chosen salts were KCl (85% R.H.), NaNO₂ (60% R.H.), and MgCl₂ (32% R.H.). All salts were dissolved in water, and the amount of water was chosen according to the

solubility of the salts to ensure that the solution contained an appropriate amount of salt to maintain the humidity inside the desiccator. The desiccators were placed in a temperature-controlled room to maintain a stable temperature of 25 °C during the experiment. Temperature and humidity were monitored regularly with a humidity meter and a thermometer placed inside the desiccator. The samples were withdrawn in a 24-hour time interval and their mechanical properties were immediately measured. The measurement of each sample was repeated five times. The samples were kept in a desiccator with the appropriate salt that maintained relative humidity, and they were removed directly before the measurement. Relative humidity and temperature were monitored during the storage of samples with a DT-172 temperature and humidity data logger by CEM (China). All measurements were made at 20 °C and 50% of relative humidity.

2.2.5. Differential scanning calorimetry

The DSC measurements were performed on a Discovery DSC from TA Instruments (USA). The sample (weighing approximately 3-5 mg) was weighed in a covered aluminum pan (40 µl). Nitrogen was used as a purge gas during the experiments. The investigation was carried out in the temperature range from 0 °C to 300 °C with a heating rate 5 °C/min (Amplitude = 0.8 °C; Period = 60 s). The enthalpy is given in J/g.

2.2.6. X-ray diffraction

To ensure the stability of the Tadalafil crystal structure during processing and consequent storage, the X-ray diffraction measurement was done using a PANalytica X'Pert³ powder diffractometer from Malvern (UK). The results obtained were compared with the diffractogram of the original drug in powder form. The copper electrode was used for the measurement with a wavelength equal to 1.54 Å.

2.2.7. The purity of samples

Tadalafil can decompose into byproducts when exposed to stress conditions, so the samples were tested for chemical purity. This was done to ensure that both the lamination and the preparation process did not lead to any chemical changes in the film. The High-Performance Liquid Chromatography (HPLC) Alliance 2695 by Waters Corporation (USA) was used for this measurement. The mobile phase A was a mixture of 1 ml of trifluoroacetic acid and 1000 ml of water, while the mobile phase B was acetonitrile. The samples were prepared by dissolving 100 mg of the sample in 250 ml of solvent. The samples were sonicated for 20 min and the undissolved material was removed by centrifugation for 10 min at 100,000 RPM. The reference solution was prepared by dissolving 20 mg of Tadalafil in 50 ml of solvent. The solution was ultrasonicated for 10 min. The measurements were performed in column Zorbax SB C8 by Agilent (USA) as a stationary phase. The temperature was maintained at 40 °C.

2.2.8. Film disintegration experiment

We could not rely on standard techniques to determine the disintegration time as our films completely disintegrated in a matter of seconds. Therefore, the experimental setup shown in Figure 2 was developed within the framework of this work. It consists of a video microscope equipped with a high-speed camera (Pixelink PL-725MU-T by Navitar, USA) and a Petri dish with a diameter of 9 cm used as a media reservoir (using always 30 ml of media). This setup provided contact of the film with the liquid and allowed observing a large area of the film for disintegration time detection. The amount of the sample with dimensions 25.0×32.0 mm was always around 60 mg, containing 18.5 mg of Tadalafil.

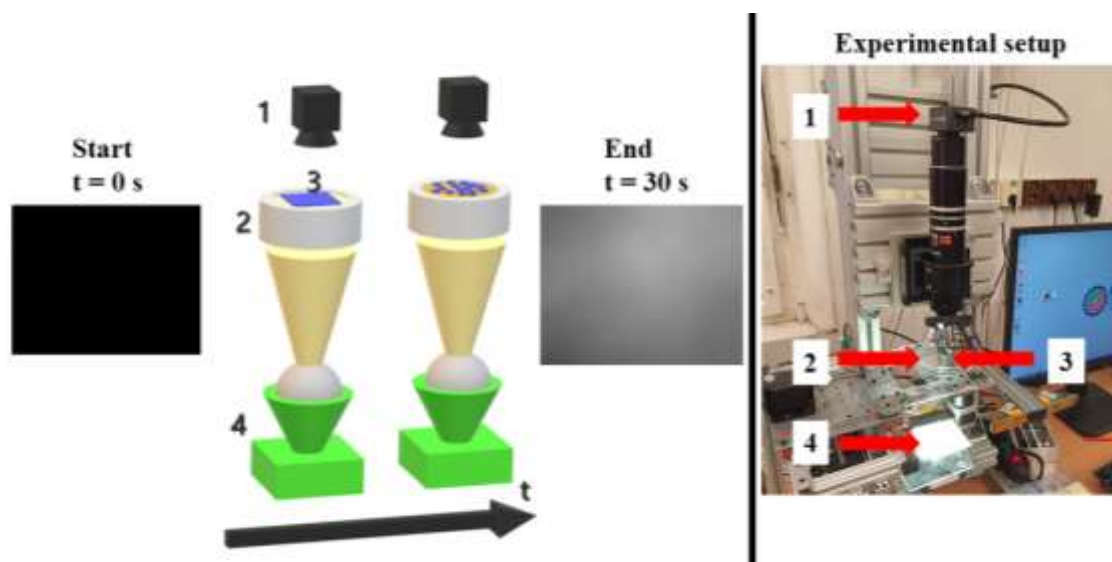


Figure 2- Schematics of the disintegration experiment. Unit 1 represents a high-speed camera. Unit 2 stands for a Petri dish with a dissolution medium. Unit 3 is a measured sample. Unit 4 is a light source. At the start of the experiment, no light is passing through. At the end of the experiment, the camera is detecting light. The endpoint (in this case, $t = 30$ s) illustrates the end of the experiment, not the disintegration time. The picture of the experimental setup is included in the right part of the image.

This setup was selected to prevent the film sample from flowing out of the field of view and to minimize the optical disturbance with the high liquid level in the Petri dish. The ODF sample was gently placed on the liquid surface while consequently being captured by the high-speed camera at a rate of 70 FPS. Since the film prevents light from passing through, the time necessary for film disintegration could be determined by monitoring the light intensity detected by the high-speed camera. The experiments were repeated three times, and the reported values corresponded to the average values. The images were further analyzed to obtain the disintegration time with ImageJ software.

To ensure that only disintegration takes place in the first few minutes, the amount of dissolved Tadalafil was measured with a Cary 60 UV/Vis spectrophotometer by Agilent (USA). A small amount of the sample was removed from the dissolution vessel followed by filtration through a $0.45 \mu\text{m}$ PTFE filter. Consequently, 1.0 ml of the filtrate was diluted with

1.0 ml of the dissolution medium and measured. All samples were stored at 20 °C and 50% of relative humidity before measurement.

The medium was prepared by mixing 17.9 ml of aqueous potassium dihydrogen phosphate solution (KH_2PO_4) with a concentration of 50 mM and 9.0 ml of aqueous sodium hydroxide solution (NaOH), which was added to the medium having a concentration of 20 mM. The acidity was checked using a SevenCompact pH meter by Mettler Toledo (CH).

2.2.9. Dissolution kinetics and evolution of particle size during dissolution

Based on the preliminary experiment, the formation of particle agglomerates was observed. The particle size of the samples was measured by a static light scattering (SLS) technique employing Mastersizer 2000 (Malvern, UK). To mimic slow mixing, fluid pumping from and back to the dissolution container with 200 ml of filling volume (to approximate the volume of the stomach) through the SLS instrument using a 120 ml syringe driven by a VIT-FIT programmable syringe pump from Lambda Instruments (Czech Republic) set at 1.2 ml/s was used. The total period between filling and emptying of the syringe was 2 minutes (1 minute for filling and 1 minute for emptying). Furthermore, to ensure permanent suspension of particles, pumping was used during which the samples were measured every 2 minutes. Because the formation of large agglomerates was observed during the preliminary experiments, the samples were also characterized with an optical microscope. A small amount of sample from the dissolution container was withdrawn and analyzed by optical microscopy to characterize the size and morphology of the formed agglomerates. In addition to the particle size, the evolution of the concentration was also measured within this experiment. The measurement was performed in 1, 2, 5, 10, and 20 minutes after the start of the dissolution experiment. The sample with a volume of 2 ml was withdrawn from the solution and filtered with a PTFE filter with a pore size of 0.45 μm . The aqueous solution for the experiments was that same as the previously mentioned. The UV/Vis spectrophotometer

was a Cary 60 from Agilent (USA) using a wavelength of 291 nm. All measurements were made in triplicates. The dissolution medium was a buffer solution with pH 2.0, and it was maintained at 37 °C and mixed at 300 RPM using a magnetic stirrer. The dimensions of the samples were 25×32 mm with a weight of 60 mg, containing 18.54 mg of Tadalafil.

Dissolution experiments from the liberated drug particles were carried out in 800 ml of buffer with pH 6.8. The medium was prepared in the same way along with the exact stirring and temperature conditions as mentioned in the previous section. The mass of the sample was set at 9.6 mg out of which Tadalafil amount was equal to 2.97 mg. This dose corresponds to 80% of solubility in the volume of water. During sampling, 2 ml of liquid was withdrawn with a syringe and filtered through a 0.45 µm PTFE filter. The samples were withdrawn at 1, 2, 5, 10, 20, 30, and 40 minutes and measured with UV/Vis Cary 60 by Agilent (USA) using a wavelength of 291 nm. The experiment was carried out in triplicates for all samples.

3. Results and discussion

3.1. Scanning electron microscopy

The summary of the SEM images obtained for laminated and non-laminated samples is shown in Figure 3, together with the distribution of the fiber diameters.

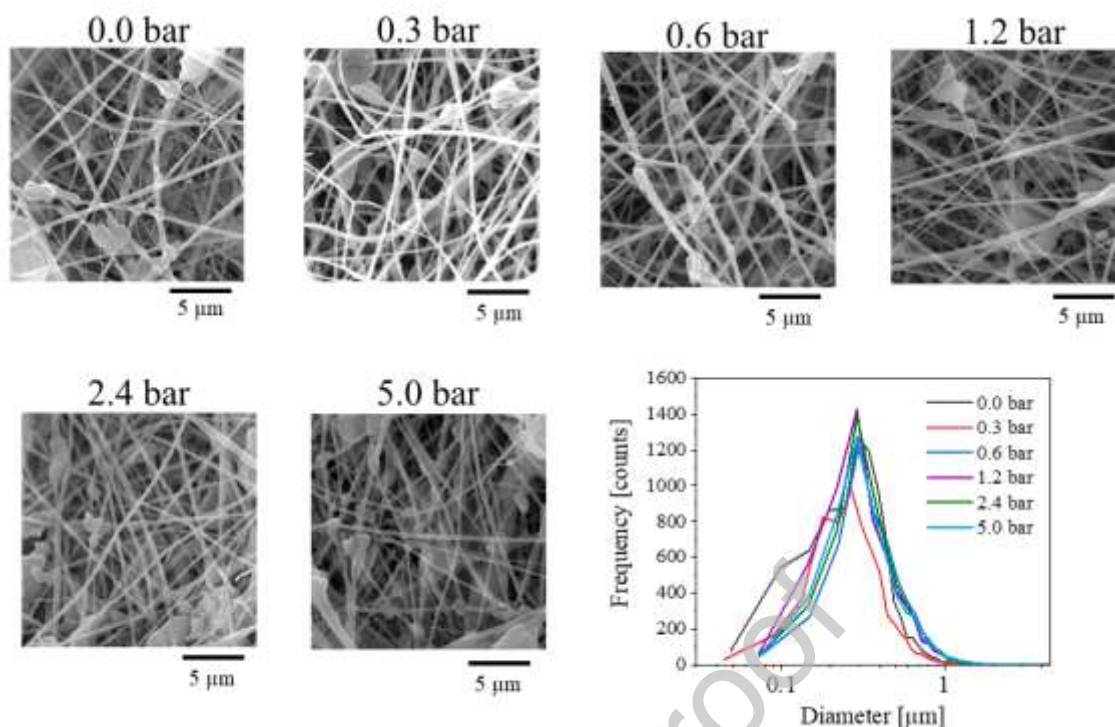


Figure 3 - SEM images of the fiber structure of the non-laminated and laminated samples using the pressure of 0.3, 0.6, 1.2, 2.4, and 5.0 bar. The black scale bar represents 5 μm. A comparison of the nanofiber diameter is also included in the figure.

As can be seen, formed nanofibers in all samples are visible together with the microparticles of Tadalafil (the round particles embedded inside the nanofibers). Despite the applied lamination pressure, the mean fiber diameter remained to be about 300 nm, with the distribution covering a range from about 50 nm up to 1 micron. Small differences were observed for the nonlaminated samples; see Figure 3, the distribution was slightly broader with a larger fraction of fibers having a diameter between 100 and 200 nm. This indicates that by applying the lamination pressure the narrowest fibers merged with the surrounding matrix and became invisible. Overall, we can conclude that this effect is not significant, and the lamination pressure did not dramatically affect the structure of the produced films.

The diameter of Tadalafil particles was analyzed by a random selection of particles from the taken images. The selection was done from five independent images and around 30 particles

were selected from each image. The results are presented in Table 3. The measured results do not demonstrate any effect of the electrospinning and lamination on the size of Tadalafil particles having a mean particle diameter of 5 microns.

Table 3 – The average diameter of the Tadalafil particles in samples.

Sample	Lamination Pressure	Diameter
[-]	[bar]	[μm]
1	0.0	4.3 ± 3.0
2	0.3	5.9 ± 2.3
3	0.6	5.1 ± 2.4
4	1.2	5.6 ± 3.0
5	2.4	6.0 ± 2.8
6	5.0	4.2 ± 1.4

3.2. Mechanical properties

The corresponding Young's modulus was obtained from the linear part of the curve as indicated by the box following the modified ISO 1924-20 using the 0.15 to 0.30 % of the strain. A similar approach was employed for other samples. A different interval from 0 to 0.30 % was used for the samples laminated at a pressure of 5.0 bar due to their brittleness, which leads to low strain values and low number of points.

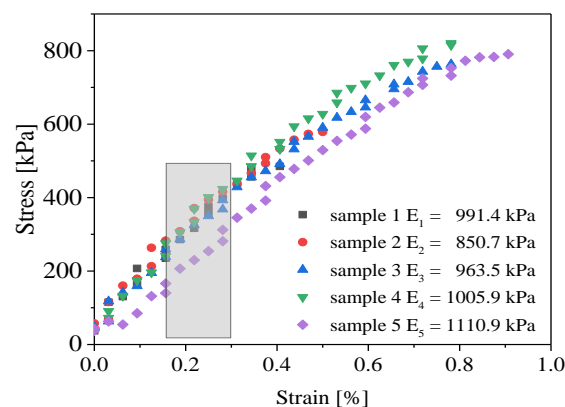


Figure 4 – The example of obtaining the stress-strain curve for the determination of the Young's modulus for the non-conditioned sample laminated with a pressure of 1.2 bar. The samples were stored at laboratory conditions (25 °C and 50% relative humidity). Each curve

was fitted with a linear trend line in an area between 0.15 % and 0.30 % of the strain (the method was based on modified ISO 1924-2 and indicated by the gray box) to obtain the value of Young's modulus. The slope of the trend line is the value of the Young's modulus. The example contains the values that were used to calculate the average value of the sample laminated by the pressure of 1.2 bar.

The results of the measured mechanical properties for the non-laminated and laminated samples prepared at pressures of 1.2, 2.4, and 5.0 bars are presented at the Table 4. Please note that samples laminated at pressures of 0.3 bar and 0.6 bar were excluded from the measurement because they delaminated during the preparation. The mentioned Young's modulus was calculated as an average value of at least five independent measurements. As it is evident from the Table 4, the Young's modulus increases with an increase in lamination pressure, which indicates greater sample stiffness. However, another important parameter for the process ability is the maximum strain, which the film can resist. As seen in Table 4, the increase of the maximum strain between the non-laminated sample and the sample laminated at a pressure of 1.2 bar was first observed, followed by a significant drop of the maximum strain down to 0.31% for the sample laminated at a pressure of 5.0 bar. This suggests that the samples became brittle. This observed maximum implies the existence of an optimal lamination pressure and an improvement of the mechanical properties.

Table 4 – The results of the Young's modulus measured for the samples laminated by different pressures.

Lamination pressure (bar)	Average Young modulus (MPa)	Maximum stress (MPa)	Maximum strain (%)
0.0	0.93 ± 0.11	0.76	0.78
1.2	0.98 ± 0.11	0.82	0.91
2.4	1.02 ± 0.07	0.47	0.66
5.0	1.23 ± 0.09	0.45	0.31

The film mechanical properties are important when considering the processability of the film for large-scale production. More elastic films might be broken during the manipulation. The values of the Young's modulus measured for the samples in this work are comparable to the values reported in the literature for electrospun films composed of HPMC and polyethylene glycol; covering the range from 0.54 MPa to 2.1 MPa (Ghosal et al., 2018).

3.2.1. The impact of conditioning on mechanical properties

Because ODFs can rapidly disintegrate in contact with water, they are also sensitive to the differences in humidity during storage. To investigate whether the observed maximum in mechanical strain will persist during the ODFs storage, the prepared samples were conditioned at various values of relative humidity. As shown in Figure 5, the observed maxima in the measured stress for the lamination pressure of 1.2 bar persist for all applied relative humidity. However, the change was highest for samples conditioned at 85% and 25 °C, with measured values of the Young's modulus increasing towards those measured for the solvent casted samples. This increase was probably caused by the water acting as a plasticizer for the polymer matrix. More water vapor leads to higher changes in the mechanical

properties, while the changes for samples conditioned at 30% and 50% were rather low resulting in similar values of maximum stress.

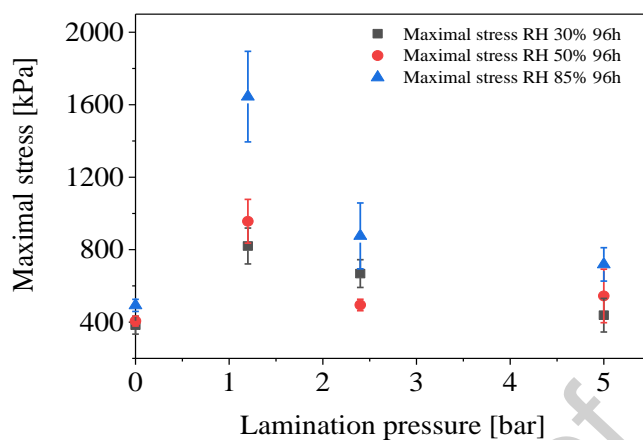


Figure 5 – The maximum stress measured during the experiment. The plot shows the average value of the maximum stress that was measured as a function of the lamination pressure. Each point was constructed from five separate measurements. The measured data for the different values of relative humidity show values for the samples conditioned for 96 h.

3.3. Differential scanning calorimetry

The results of the DSC measurement are shown in Figure 6. As can be seen, there is no significant difference between the samples laminated at various pressures. The measured peaks were on similar positions for all samples and corresponded to the melting of PEG 100 000 ($T_{p1} = 52\text{ }^{\circ}\text{C}$) and the recrystallization and the melting of sucrose ($T_{p2} = 179\text{ }^{\circ}\text{C}$, $T_{p3} = 210\text{ }^{\circ}\text{C}$). The latter was found to agree with the literature (Beckett et al., 2006). The last peak corresponds to the melting of Tadalafil ($T_{p4} = 265\text{ }^{\circ}\text{C}$). HPMC E5 was not visible during the measurements due to its amorphous phase. This confirms that no phase changes occurred inside the sample during lamination. Therefore, in the case of the studied polymer mixture and the drugs used, the conclusion is that the electrospinning and the consequent lamination process have any negative effect on the chemical purity of the prepared samples.

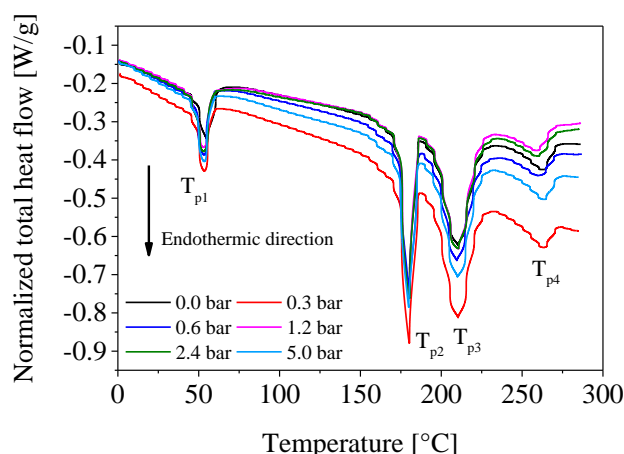


Figure 6 - DSC curves for all samples. The peaks correspond to the melting of PEG 100 000 ($T_{p1} = 52$ °C), the recrystallization and melting of sucrose ($T_{p2} = 179$ °C, $T_{p3} = 210$ °C), and the melting of Tadalafil ($T_{p4} = 265$ °C).

3.4. X-Ray diffraction

The diffractograms of all the samples are compared in Figure 7. The sample laminated at a pressure of 0.3 bar was excluded because it delaminated during the manipulation, preventing further analysis of the layers. In contrast, even though the sample laminated by the pressure of 0.6 bar delaminated, the layers remained separable and analyzable.

As it is evident from the measured diffractograms, the characteristic peaks for Tadalafil did not change. Thus, no solid-state transformation of the API was supported during electrospinning nor during lamination. One of the differences observed between the samples corresponds to a small change for the 24.8° and 25.3° positions, corresponding to the signal from crystalline sucrose (see Figure 7 part G). There was no difference between the relative intensity of these peaks for laminated pressure of 0.6 and 1.2 bar, while the relative intensity of the peaks at 24.8° and 25.3° changed when the films were laminated at a higher pressure. This suggests that the solid-state sucrose might have changed from crystalline to amorphous state when applying higher lamination pressures, i.e. 2.4 and 5 bar (Ridgway et al., 1969).

This could explain the fragility of the sample that was observed in the measurement of the mechanical properties.

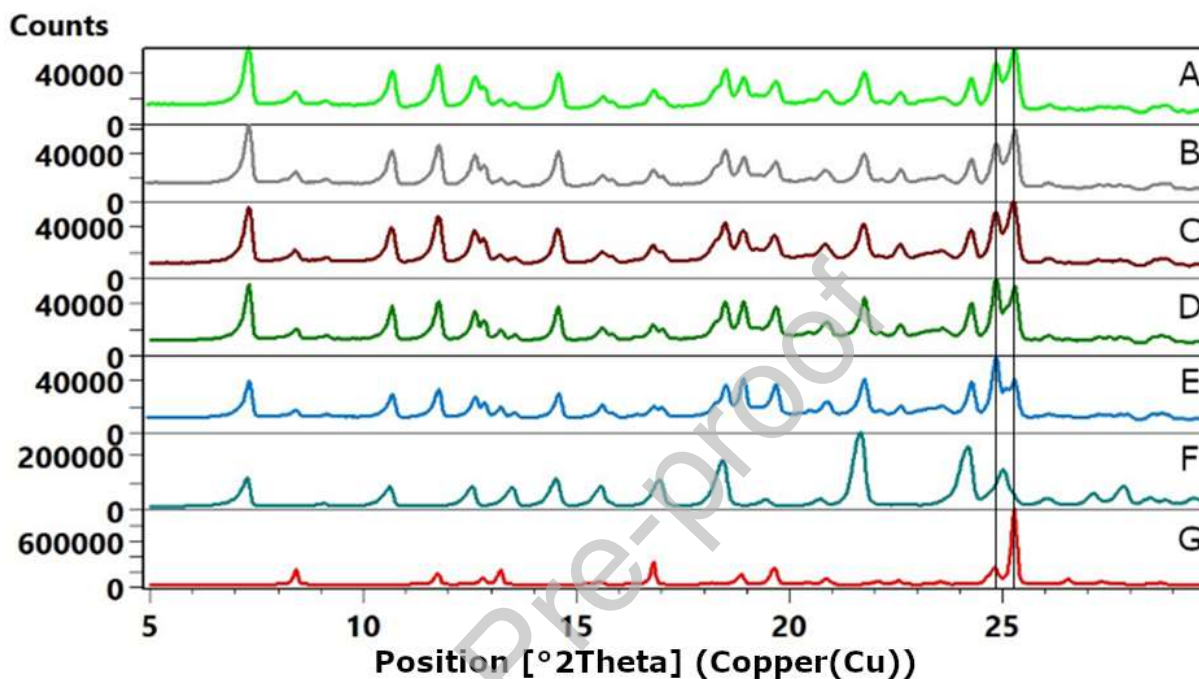


Figure 7 – The samples measured with the XRD different laminated pressures: 0.6 bar outer layer (A), 0.6 bar inner layer (B), 1.2 bar (C), 2.4 bar (D), and 5.0 bar (E). For completeness, the XRD data for Tadalafil (F) and (G) sucrose as the most abundant components of ODF were also included. The peaks of interest are indicated as vertical lines.

3.5. Purity of samples

The measurements from the HPLC analysis independently confirmed no toxic by-products from the degradation of Tadalafil. The amount of impurities determined by the HPLC analysis was below 0.03%. No measurable amount of residual organic solvents in the samples was detected. The amount of water in the samples was around 0.5%. The presence of water could be a residuum from the preparation or uptake from the atmosphere during storage. This

measurement confirmed previously measured data from the DSC analysis that the lamination pressure has no effect on the impurities in the sample.

3.6. Disintegration time

All the samples prepared within the frame of this work were able to meet the limit of 30 s as defined by the European Pharmacopoeia (EDQM, July 2019). When testing the available methods for film disintegration, no available method in the literature was found suitable for the measurement of the fast-disintegrating films prepared in this work. The preliminary experiments of the disintegration time observed for the samples prepared in this work are significantly shorter than 30 s; hence, a new method for measuring the disintegration time was developed. The measurement was done in 30 ml of solution. The volume of fluid is larger than what would normally be presented in the mouth cavity; however, this volume was chosen to allow the measurement of drug dissolution during the disintegration process that takes place in the mouth cavity. The lower volume would prevent reliable measurements of the dissolve API since the volume of the withdrawn liquid would represent the noticeable amount in respect to the total liquid volume.

The algorithm for determining the disintegration time is presented in Figure 8-A. The data are presented for one sample. The histogram of 8-bit greyscale image is obtained from the acquired images. The average value of the histograms is extracted from the images and plotted as a function of time (see Figure 8-B). The numerical derivation of the determined values is used to determine the point with the maximum change (see Figure 8-C). This was chosen as a robust method to determine the point where the samples are considered disintegrated.

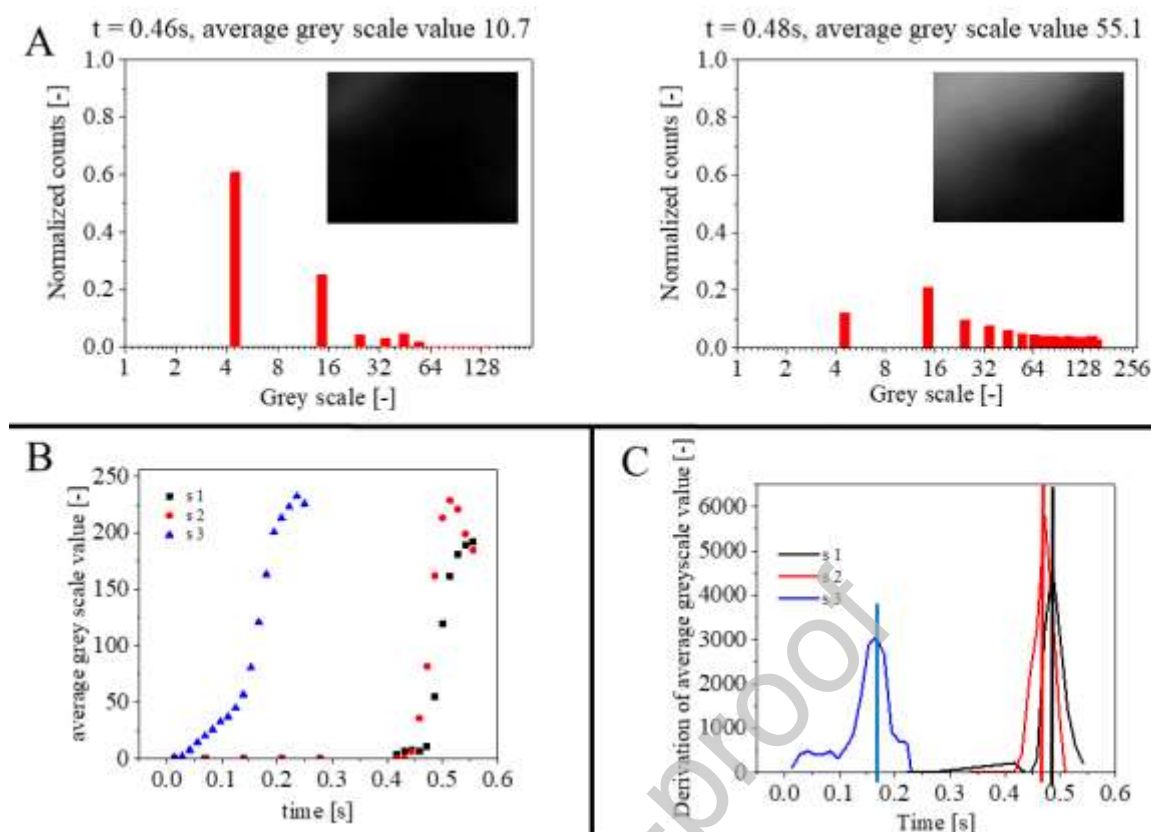


Figure 8 – An example of the data evaluation from the disintegration experiment for a non-laminated sample. The first step (A) is to get a histogram of the acquired images and calculate the average greyscale value of the histograms. The second step (B) is to plot the data, while the third step (C) is to apply the first-order numerical derivation on the plotted data. The disintegration time is determined as a point with the maximum value of the numerical derivation for the average greyscale value. The upper row shows the histograms for the sample obtained right before the sample was considered disintegrated and at the disintegrated time. The example includes the data obtained for a sample laminated by the pressure of 0.0 bar. The points mark as s1, s2, s3 in panels 1 and 2, stand for samples 1, 2 and 3. The samples represent the repetition of the experiment.

The fastest time was 0.4 s for a non-laminated sample. On the contrary, the longest observed disintegration time was around 12 s for a sample laminated at a pressure of 5.0 bar. This time is well below the limit set for the orally disintegrable films. These findings clearly indicate the advantage of the fast-disintegrating ODFs prepared by electrospinning. The results confirmed the assumption that the compression of the structure would increase the density of the material, and thus prolong the disintegration time.

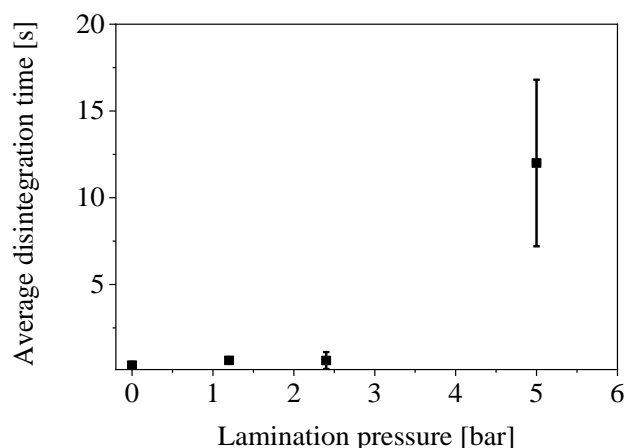


Figure 9 – The time of disintegration as a dependence and lamination pressure. The error bars indicate the reproducibility of the measurement. The measurement of each sample was performed in triplicate.

The analysis of the dissolved drug was performed during the disintegration process to ensure that the disintegration time was not affected by potential fast drug dissolution. The samples were taken from the same container as used for determining the disintegration time. As illustrated in Figure 10, the amount of dissolved drug during ODF disintegration is minute and remains constant after 2 min. Furthermore, no significant difference was observed between all the laminated samples. The constant values were obtained at the steady state, where the amount of dissolved drug was equal to only $0.22\pm 0.03\%$ of the declared dose, thus not affecting the disintegration process.

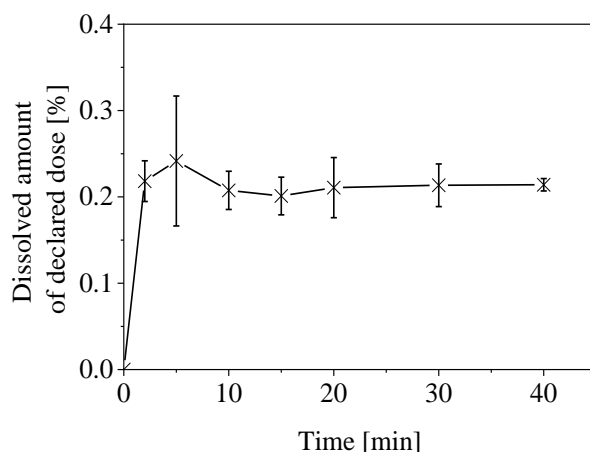


Figure 10 – The determination of the dissolved drug amount during and shortly after the film disintegration measured in 30 ml of the media with $\text{pH} = 6.8$. Due to the similar time profiles measured for different lamination pressures, the presented values were obtained by averaging the measured values for all samples laminated at different pressures. The error bars indicate the amount of variation of the dissolved drug at the given time obtained for all laminated pressures.

3.7. Dissolution kinetics and evolution of particle size during dissolution

Although disintegration is essential for film quality (Silva et al., 2018; Speer et al., 2018), the API dissolution kinetics is important when considering the therapeutic effect. This is of particular importance when considering samples with APIs in the form of particles.

The time that the disintegrated film spends in the mouth cavity is relatively short, particularly in the order of a few seconds. In what follows, the drug dissolution was measured under various conditions approximating non-sink conditions at lower pH as present in the stomach and under sink conditions (using media volumes of 800 ml), typically used for dissolution testing.

Since the prepared formulation of the ODFs contained particles, which after the liberation might have aggregated, and thus negatively affected the kinetics of the dissolution, in what follows, the behavior of the particles at reduced pH was investigated. To do so, a 200 ml dissolution vessel was used. This volume was considered as an approximation of the volume

of the stomach. The summary of the obtained results is presented in Figure 11. As can be seen, despite the ODFs lamination, an evolution of two particle populations was visible, where the small particles with an average diameter of about 5 μm corresponded to the original particle sizes of Tadalafil used for electrospinning (see Table 3). This population disappeared with time, while the second population of bigger particles started growing. This suggests that the original micronized Tadalafil particles, once released from the nanofibers, begin to form larger aggregates (EDQM, July 2019).

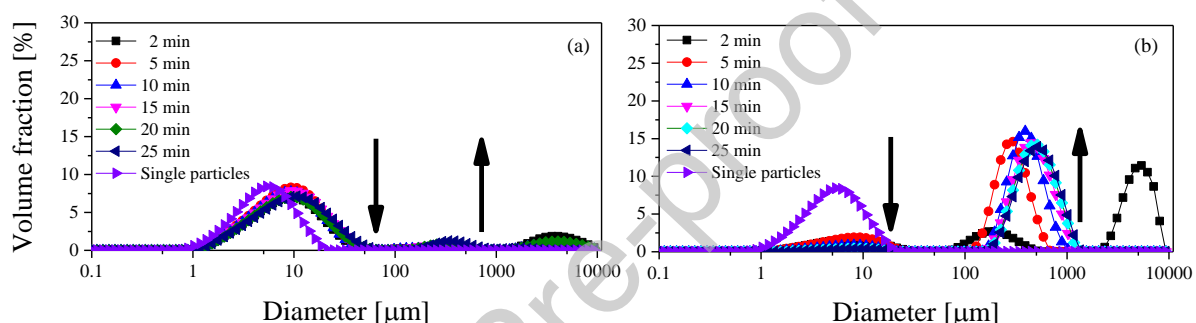


Figure 11 -The evolution of particle population in time for samples laminated by the pressure of 0.0 bar (a), 5.0 bar (b). The total volume of the liquid in a beaker, a connective tubing, a syringe for the pumping, and a measuring cell adds to 200 ml of solution. The presented samples were measured at pH 2.0. The measurement for other samples and the pH value are presented in the supplementary material.

To verify the existence of the second population and to characterize the morphology of the formed particles, optical microscopy was performed at various times as seen in Figure 12. The captured images confirmed the presence of small individual particles with a diameter of about 5 μm , which is in agreement with the particle analysis present in Table 3, together with larger fractal-like aggregates of size ranging from 70 μm to 150 μm . The size of these fractal-like aggregates is in good agreement with those measured by laser diffraction (see Figure 11), confirming the validity of both measurements. This supports the hypothesis that Tadalafil

particles upon disintegration of the ODF and dissolution of the soluble excipients undergo aggregation. However, based on the measured kinetics, it can be assumed that the suspension reaches the stomach smoothly because the aggregates begin to form after 5 minutes. The observed trends are similar to those measured for other lamination pressures. The complete data set for the physical mixture and other lamination pressures is presented in the supplementary material (see Figure SI 3 in the supplementary material).

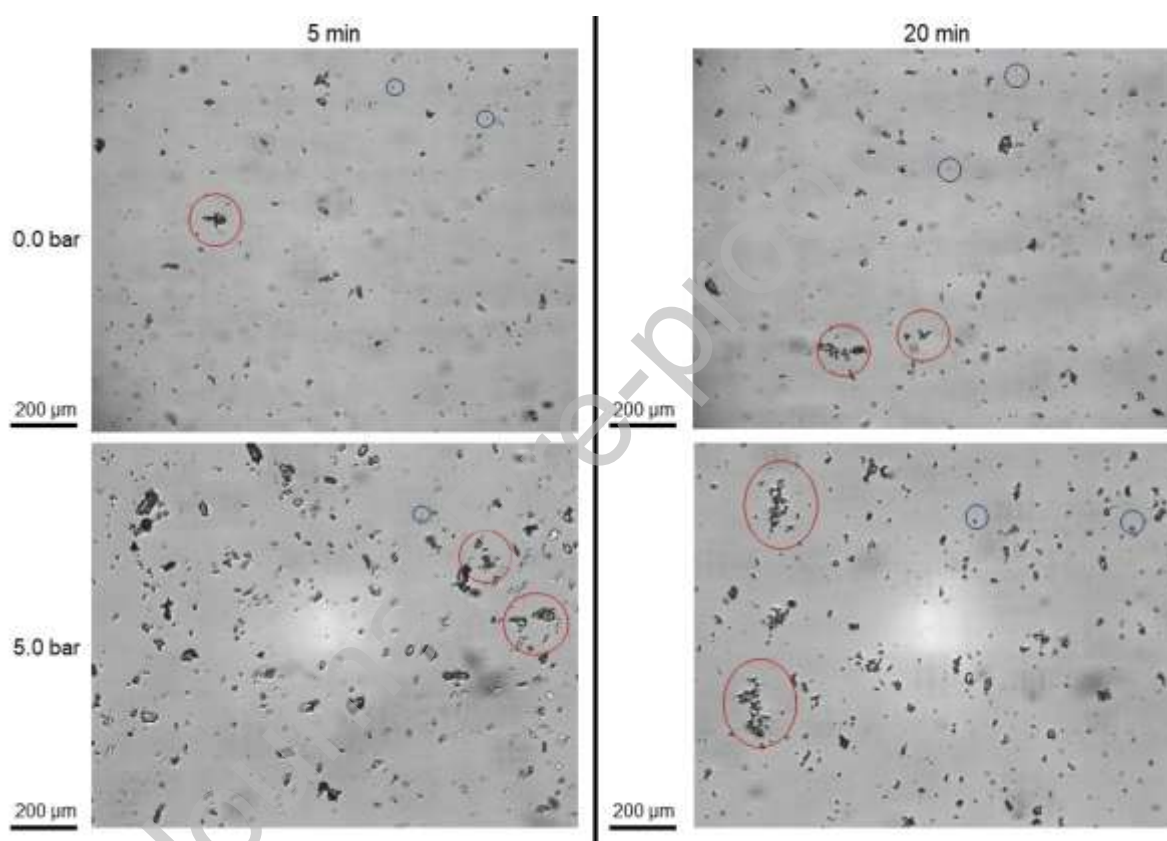


Figure 12 - Images from an optical microscope. The measurements are done for a non-laminated sample and a sample laminated at a pressure of 5.0 bar. The two columns show 5 min after the start of the experiment and 20 min after the start of the experiment. The red circles show objects identified as clusters of particles while the blue circles indicate individual small particles. The scale bar is the same for all the images since the microscope settings were identical between experiments.

The measurement of the drug concentration in the media was performed as a function of time to observe the impact of aggregation on the Tadalafil dissolution kinetics, since aggregation could negatively impact dissolution. As can be seen in Figure 13, when considering the error

bars of the measurement, it was concluded that the effect of the lamination on the time evolution of the Tadalafil concentration is negligible and the dissolved amount reached the values equal to 4.01 ± 0.42 %. Similar to the results present in Figure 10, the measured values are independent of the applied lamination pressure. Furthermore, the higher amount of dissolved Tadalafil compared to those shown in Figure 10 suggest that the amount of the dissolved drug is only a function of media volume. In addition, the measured kinetics confirmed no impact of aggregation, which can be attributed to the open structure of fractal-like aggregates as illustrated in and thus no limitation for drug diffusion.

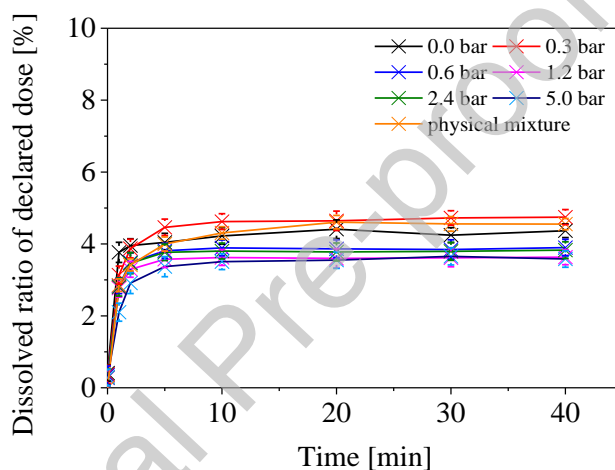


Figure 13 - Dissolution kinetics of API. The measurements were done in a beaker using a media volume of 200 ml. The medium was a buffer solution with $\text{pH} = 2.0$.

Additional dissolution experiments were performed in 800 ml volume using sink conditions to confirm that the amount of dissolved drug is only a function of the used media volume. As can be seen in Figure 14, the amount of dissolved drug reached 80 % in 40 min with no influence of the lamination pressure on the dissolution kinetics, confirming that there is no limit for the removal of particles from the polymeric matrix. In addition, the electrospun fibers had a positive effect on the dissolution kinetics compared to the dissolution of a pure drug or a physical mixture. This improved effect is attributed to the fast dissolution of

polymer fibers, which occurs when the material is in contact with water, thus enhancing the dissolution kinetics of the drug. Furthermore, according to the Handbook of Pharmaceutical Excipients Ninth Edition (Sheskey et al., 2020), both HPMC and PEG can enhance the solubility of drugs. Long-term measurements were also performed for all laminated samples to ensure that all the drug content would be released and dissolved. All samples reached 100% of the dissolved ratio of declared dose after 24 h. The Tadalafil concentration was at this point 3.6 mg/l. This shows that after a sufficient amount of time, all the drug content was released.

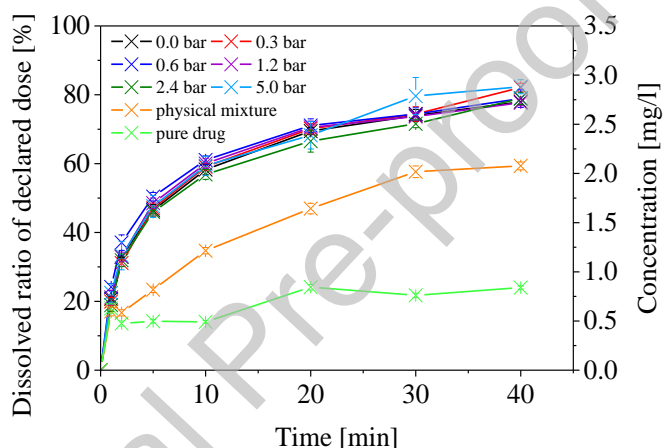


Figure 14 - The evolution of the dissolved drug concentration for the samples dissolved in a buffer with pH = 6.8. The right y-axis shows the measured concentration of the solution, while the left y-axis indicates the dissolved percentage of Tadalafil

Based on these results, it was concluded that lamination has no impact on the dissolution profile irrespectively of the dissolution media amount or the amount of used API sample. This is due to the very fast disintegration of the film, after which the dissolution process is controlled by the dissolution of the drug from individual particles. The presented data indicate that the produced formulation allows the dynamics of the disintegration and the drug dissolution, which can be adjusted according to the optimal therapeutic profile for the patient. In particular, this can be easily achieved by changing the size of the used API particles

without any modification of the electrospinning process or the matrix composition. Compared to the tablets, such decoupling is often not possible since disintegration in the case of tablets is typically in the order of minutes and not seconds as it is for ODFs prepared in this work.

4. Conclusion

In this research, the possibility of preparing nanofibrous orally dispersible films (ODFs) by electrospinning using particle dispersion of a model drug Tadalafil was examined. Since ODFs are made up of nanofibers, which are rather fragile during handling, the impact of lamination and conditioning was tested under various levels of relative humidity. No differences were observed between the samples measured by SEM and DSC for all lamination pressures, covering a range from 0 to 5 bar. The XRD measurement showed a difference in a sample laminated with the pressure above 2.4 bar, where a partial decrease in crystalline sucrose was observed. No significant differences were also observed during the measurements of the dissolution kinetics and the measurement of the drug particles during the dissolution. This shows that the lamination pressure does not have a significant effect on the sample composition and structure. A significant difference was observed in the disintegration time, suggesting a possible compaction of the inner nanofiber film structure, supported by the increase in Young's modulus measured for samples laminated at a higher pressure. However, when considering the processability, which is related to the stress-strain characteristic, we observed the maximum stress for samples laminated by the pressure equal to 1.2 bar. This suggests that when material processing and packaging will be considered, the optimum lamination pressure around 1.2 bar would provide the best mechanical properties for the produced ODFs.

5. Acknowledgment

This work was supported by the specific university research grant No A1_FCHI_2021_005 and by the Pharmaceutical Applied Research Center (PARC).

Credit Author Statement

Dominik Švára – Conceptualization, Methodology, Investigation, Data Curation, Writing - Original Draft, Writing – Review & Editing, Visualization

Barbora Kopřivová – Methodology, Investigation, Writing - Original Draft

Tomáš Pícek – Investigation

Petr Mikeš – Supervision, Writing – Review & Editing, Resources

Anna Kluk – Conceptualization, Resources, Writing – Review & Editing, Supervision

Miroslav Šoos – Conceptualization, Writing – Review & Editing, Supervision

6. References

Akhgari, A., Shakib, Z., Sanati, S., 2017. A review on electrospun nanofibers for oral drug delivery. *Nanomedicine Journal* 4, 197-207.

Alomari, M., Mohamed, F.H., Basit, A.W., Gaisford, S., 2015. Personalised dosing: printing a dose of one's own medicine. *International Journal of Pharmaceutics* 494, 568-577.

Alomari, M., Vuddanda, P.R., Trenfield, S.J., Dodoo, C.C., Velaga, S., Basit, A.W., Gaisford, S., 2018. Printing T3 and T4 oral drug combinations as a novel strategy for hypothyroidism. *International Journal of Pharmaceutics* 549, 363-369.

Arinstein, A., 2017. *Electrospun polymer nanofibers*. CRC Press.

Beckett, S.T., Francesconi, M.G., Geary, P.M., Mackenzie, G., Maulny, A.P., 2006. DSC study of sucrose melting. *Carbohydrate Research* 341, 2591-2599.

Borges, A.F., Silva, C., Coelho, J.F., Simões, S., 2015. Oral films: current status and future perspectives: I—galenical development and quality attributes. *Journal of Controlled Release* 206, 1-19.

- Buanz, A.B., Belaunde, C.C., Soutari, N., Tuleu, C., Gul, M.O., Gaisford, S., 2015. Ink-jet printing versus solvent casting to prepare oral films: Effect on mechanical properties and physical stability. *International Journal of Pharmaceutics* 494, 611-618.
- Buanz, A.B., Saunders, M.H., Basit, A.W., Gaisford, S., 2011. Preparation of personalized-dose salbutamol sulphate oral films with thermal ink-jet printing. *Pharmaceutical Research* 28, 2386-2392.
- Bukhary, H., Williams, G.R., Orlu, M., 2018. Electrospun fixed dose formulations of amlodipine besylate and valsartan. *International Journal of Pharmaceutics* 549, 446-455.
- Cheng, L., Wang, Y., Sun, G., Wen, S., Deng, L., Zhang, H., Cui, W., 2020. Hydration-enhanced lubricating electrospun nanofibrous membranes prevent tissue adhesion. *Research* 2020.
- Dvořák, J., Tomas, J., Lizoňová, D., Schöngut, M., Dammer, O., Pekárek, T., Beránek, J., Štěpánek, F., 2020. Investigation of tablet disintegration pathways by the combined use of magnetic resonance imaging, texture analysis and static light scattering. *International Journal of Pharmaceutics* 587, 119719.
- EDQM, E.P., July 2019. *European Pharmacopoeia*, 10th ed. Council of Europe, B.P. 907, F - 67029, Strasbourg, France
- Feng, X., Hou, X., Cui, C., Sun, S., Sadik, S., Wu, S., Zhou, F., 2021. Mechanical and antibacterial properties of tannic acid-encapsulated carboxymethyl chitosan/polyvinyl alcohol hydrogels. *Engineered Regeneration* 2, 57-62.
- Ghosal, K., Chandra, A., Praveen, G., Snigdha, S., Roy, S., Agatemor, C., Thomas, S., Provaznik, I., 2018. Electrospinning over solvent casting: tuning of mechanical properties of membranes. *Scientific Reports* 8, 1-9.
- Hoffmann, E.M., Breitenbach, A., Breitreutz, J., 2011. Advances in orodispersible films for drug delivery. *Expert Opinion on Drug Delivery* 8, 299-316.
- Hotaling, N.A., 2016. DiameterJ, Available from: <https://imagej.net/DiameterJ>.
- Hotaling, N.A., Bharti, K., Kriel, H., Simon Jr, C.G., 2015. DiameterJ: A validated open source nanofiber diameter measurement tool. *Biomaterials* 61, 327-338.
- Illangakoon, U.E., Gill, H., Shearman, G.C., Parhizkar, M., Mahalingam, S., Chatterton, N.P., Williams, G.R., 2014. Fast dissolving paracetamol/caffeine nanofibers prepared by electrospinning. *International Journal of Pharmaceutics* 477, 369-379.
- Jani, R., Patel, D., 2015. Hot melt extrusion: An industrially feasible approach for casting orodispersible film. *Asian Journal of Pharmaceutical Sciences* 10, 292-305.
- Lang, B., McGinity, J.W., Williams III, R.O., 2014. Hot-melt extrusion—basic principles and pharmaceutical applications. *Drug Development and Industrial Pharmacy* 40, 1133-1155.
- Li, X., Kanjwal, M.A., Lin, L., Chronakis, I.S., 2013. Electrospun polyvinyl-alcohol nanofibers as oral fast-dissolving delivery system of caffeine and riboflavin. *Colloids and Surfaces B: Biointerfaces* 103, 182-188.

- Lian, H., Meng, Z., 2017. Melt electrospinning vs. solution electrospinning: A comparative study of drug-loaded poly (ϵ -caprolactone) fibres. *Materials Science and Engineering: C* 74, 117-123.
- Lukas, D., Sarkar, A., Pokorny, P., 2008. Self-organization of jets in electrospinning from free liquid surface: A generalized approach. *Journal of Applied Physics* 103, 084309.
- Mikeš, P., Brož, A., Sinica, A., Asatiani, N., Bačáková, L., 2020. In vitro and in vivo testing of nanofibrous membranes doped with alaptide and L-arginine for wound treatment. *Biomedical Materials* 15, 065023.
- Nagy, Z.K., Nyúl, K., Wagner, I., Molnár, K., Marosi, G., 2010. Electrospun water soluble polymer mat for ultrafast release of Donepezil HCl. *Express Polymer Letters* 4, 763-772.
- Nieminen, H.J., Laidmäe, I., Salmi, A., Rauhala, T., Paulin, T., Heinämäki, J., Hægström, E., 2018. Ultrasound-enhanced electrospinning. *Scientific Reports* 8, 1-6.
- Oliveira, J.E., Mattoso, L.H., Orts, W.J., Medeiros, E.S., 2013. Structural and morphological characterization of micro and nanofibers produced by electrospinning and solution blow spinning: a comparative study. *Advances in Materials Science and Engineering* 2013.
- Orlu, M., Ranmal, S.R., Sheng, Y., Tuleu, C., Seddon, P., 2017. Acceptability of orodispersible films for delivery of medicines to infants and preschool children. *Drug Delivery* 24, 1243-1248.
- Pechová, V., Gajdziok, J., Muselík, J., Vetchý, D., 2018. Development of orodispersible films containing benzydamine hydrochloride using a modified solvent casting method. *AAPS PharmSciTech* 19, 2509-2518.
- Preis, M., 2015. Orally disintegrating films and mini-tablets—innovative dosage forms of choice for pediatric use. *AAPS PharmSciTech* 16, 234-241.
- Quodbach, J., Moussavi, A., Tammer, R., Frahm, J., Kleinebudde, P., 2014. Tablet disintegration studied by high-resolution real-time magnetic resonance imaging. *Journal of Pharmaceutical Sciences* 103, 249-255.
- Ridgway, K., Shotton, E., Glasby, J., 1969. The hardness and elastic modulus of some crystalline pharmaceutical materials. *Journal of Pharmacy and Pharmacology* 21, 19S-23S.
- Sheskey, P.J., Hancock, B.C., Moss, G.P., Goldfarb, D.J., 2020. *Handbook of Pharmaceutical Excipients* Ninth edition. Pharmaceutical Press.
- Silva, D.A., Webster, G.K., Bou-Chacra, N., Löbenberg, R.J.D.T., 2018. The significance of disintegration testing in pharmaceutical development. *Dissolution Technologies* 25, 30-38.
- Slavkova, M., Breikreutz, J., 2015. Orodispersible drug formulations for children and elderly. *European Journal of Pharmaceutical Sciences* 75, 2-9.
- Speer, I., Steiner, D., Thabet, Y., Breikreutz, J., Kwade, A., 2018. Comparative study on disintegration methods for oral film preparations. *European Journal of Pharmaceutics and Biopharmaceutics* 132, 50-61.

Vanaei, S., Parizi, M., Salemizadehparizi, F., Vanaei, H., 2021. An overview on materials and techniques in 3d bioprinting toward biomedical application. *Engineered Regeneration* 2, 1-18.

Vasvári, G., Kalmár, J., Veres, P., Vecsernyés, M., Bácskay, I., Fehér, P., Ujhelyi, Z., Haimhoffer, Á., Rusznyák, Á., Fenyvesi, F., 2018. Matrix systems for oral drug delivery: Formulations and drug release. *Drug Discovery Today: Technologies* 27, 71-80.

Visser, J.C., Eugresya, G., Hinrichs, W.L., Tjandrawinata, R.R., Avanti, C., Frijlink, H.W., Woerdenbag, H.J., 2017. Development of orodispersible films with selected Indonesian medicinal plant extracts. *Journal of Herbal Medicine* 7, 37-46.

Yarin, A., Zussman, E., 2004. Upward needleless electrospinning of multiple nanofibers. *Polymer* 45, 2977-2980.

Zeng, J., Xu, X., Chen, X., Liang, Q., Bian, X., Yang, L., Jing, X., 2003. Biodegradable electrospun fibers for drug delivery. *Journal of Controlled Release* 92, 227-231.

Journal Pre-proof